Crystal Structure and Magnetic Properties of Diaqua(L-aspartato)copper(II)

R. Calvo,*[1a,b] C. A. Steren,†[1a] O. E. Piro,[1c] T. Rojo,[1d] F. J. Zuñiga,[1d] and E. E. Castellano[1e]

INTEC (CONICET-UNL), Güemes 3450, 3000 Santa Fe, Argentina, Facultad de Bioquímica y Ciencias Biológicas, Universidad Nacional del Litoral, C.C. 530, 3000 Santa Fe, Argentina, Facultad de Ciencias Exactas, Universidad Nacional de La Plata, C. C. 67, 1900 La Plata, Argentina, Facultad de Ciencias, Universidad del País Vasco, Apartado 644, E-48080 Bilbao, Spain, and Instituto de Física e Química de São Carlos, Universidade de São Paulo, C.P. 369, 13560 São Carlos SP, Brazil

Received March 24, 1993®

The title compound, $Cu(CO_2NH_2CHCH_2CO_2)(H_2O)_2$, crystallizes in the space group $C2$, with $a = 9.504(1)$ Å, $b = 10.038(3)$ Å, $c = 7.555(1)$ Å, $\beta = 94.01°$, and $Z = 4$. The structure was solved by employing 807 independent reflections with $I > 3\sigma(I)$, by Patterson and difference Fourier techniques, and refined by full-matrix least squares to $R = 0.024$. The Cu(II) ion is in a distorted tetragonal pyramidal coordination. The shortest equatorial bonds occur at the pyramid base with a water oxygen [d(Cu–OW) = 1.946(3) Å], the nitrogen [d(Cu–N) = 1.998(4) Å], an α-carboxylic oxygen [d(Cu–O) = 1.955(3) Å] of one aspartate ion (asp), and a β-carboxylic oxygen [d(Cu–O) = 1.950(2) Å] of another aspartate ion related to the first by a c translation. The longest bond occurs with a water oxygen at the pyramid apex [d(Cu–OW) = 2.313(3) Å]. The equatorial bonding causes -asp-Cu-asp-Cu-asp- chains along c. These are linked by a network of interchain H-bonds involving the water molecules and the amino groups. Magnetic susceptibility data obtained between 5 K and room temperature show an antiferromagnetic behavior, with a peak value at about 7 K, and no indication of a phase transition to a 3D ordered magnetic phase. These data are interpreted in terms of a linear chain model, with antiferromagnetic exchange interaction of coupling constant $J/k = 5.3$ K between neighboring copper ions on a chain. The intrachain superexchange path is identified with the σ bonds along the skeleton of the aspartic acid molecule. The susceptibility data also suggest ferromagnetic exchange coupling between copper ions in different chains. Room-temperature EPR measurements at 9.7 and 33.4 GHz in single-crystal samples show a single resonance for any orientation of the applied magnetic field. It results from the collapse due to exchange interaction of the pair of resonances expected for the two magnetically nonequivalent Cu(II) sites in the unit cell. From the crystal **g**-tensor we calculate the molecular g-values of individual copper ions. These values are then related to the electronic structure around Cu(II) and compared with those obtained in related compounds. The magnetic interactions in the aspartic acid compound are discussed in terms of the superexchange paths and compared with those observed in other copper–amino acid complexes.

Introduction

Copper complexes of amino acids are of continuous interest, since they are simple model systems to study metal–protein interaction.[2,3] Also, in many cases they exhibit low-dimensional magnetic behavior, as revealed by magnetic susceptibility, EPR, and specific heat measurements.[4-8]

The bonding of copper ions with aspartic acid has been studied in solution, with added imidazole, bipyridyl, and phenanthroline ligands. These groups seem to enhance the affinity of copper for the oxygen donor sites of anionic ligands.[9,10] Also, in the solid state, mixed copper complexes of aspartic acid with imidazole, bipyridine, and phenanthroline have been characterized by spectroscopic[11-15] and X-ray structural[13-15] techniques. Antolini *et al.*[13] reported the preparation and spectroscopic, magnetic, and thermal studies of a complex of Cu(II) with L-aspartic acid. These authors suggested a tetragonally distorted square pyramidal coordination around copper, with two coordinated water molecules. They also discussed the possibility of a polymer-like structure with the amino acid molecule binding more than one metal ion, like that found in (L-glutamato) copper dihydrate.[16]

As part of our studies on magneto–structural correlations in copper–amino acid complexes, and motivated by the results of our recent investigation of (L-glutamato)copper dihydrate,[17] we performed X-ray structural, magnetic susceptibility, and powder and single-crystal electron paramagnetic resonance (EPR) studies of diaqua(L-aspartato)copper(II) [for short, $Cu(L\text{-asp})(H_2O)_2$], the compound reported by Antolini *et al.*[13] The Cu(II) ion is in a square pyramidal coordination with an aspartate ion acting as a bidentate ligand through the nitrogen and one α-carboxylate oxygen atom, a β-carboxylate oxygen of another aspartate ion, and a water oxygen, all at the pyramid base. A second water oxygen is at the pyramid apex. The complex crystallizes in a one-dimensional polymer-like structure where a pair of adjacent

† Present address: Department of Chemistry, University of Massachusetts, Boston, MA.

* Abstract published in *Advance ACS Abstracts*, October 1, 1993.

(1) (a) INTEC (CONICET-UNL). (b) Universidad Nacional del Litoral. (c) Universidad Nacional de La Plata. (d) Universidad del País Vasco. (e) Universidade de São Paulo.
(2) Freeman, H. C. *Inorganic Biochemistry*; Eichhorn, G. L., Ed.; Elsevier: Amsterdam, 1973; Chapter 3 and references cited therein.
(3) Brill, A. S. *Transition Metals in Biochemistry*; Springer Verlag: Berlin, 1977.
(4) Newman, P. R.; Imes, J. L.; Cowen, J. W. *Phys. Rev. B* **1976**, *13*, 4093.
(5) Calvo, R.; Passeggi, M. C. G.; Novak, M. A.; Symko, O. G.; Oseroff, S. B.; Nascimento, O. R.; Terrile, M. C. *Phys. Rev. B* **1991**, *43*, 1074.
(6) Levstein, P. R.; Pastawski, H. M.; Calvo, R. *J. Phys. Condens. Matter* **1991**, *3*, 1877.
(7) Wakamatsu, T.; Hashiguchi, T.; Nakano, M.; Sorai, M.; Suga, H.; Tan Zhi-Cheng *Chin. Sci. Bull.* **1989**, *34*, 1795.
(8) Siqueira, M. L.; Rapp, R. E.; Calvo, R. *Phys. Rev. B* **1993** *48*, 3257.
(9) Mohan, M. S.; Bancroft, D.; Abbot, E. H. *Inorg. Chem.* **1979**, *18*, 1527.
(10) Sigel, H. *Inorg. Chem.* **1980**, *19*, 1411.
(11) Kwik, W. L.; Ang, K. P.; Chen, G. *J. Inorg. Nucl. Chem.* **1980**, *42*, 303.
(12) Bunel, S.; Ibarra, C.; Rodriguez, M.; Urbina, A.; Bunton, C. A. *J. Inorg. Nucl. Chem.* **1981**, *43*, 967.
(13) Antolini, L.; Marcotrigiano, G.; Menabue, L.; Pellacani, G. C.; Saladini, M. *Inorg. Chem.* **1982**, *21*, 2263.
(14) Antolini, L.; Marcotrigiano, G.; Menabue, L.; Pellacani, G. C. *Inorg. Chem.* **1983**, *22*, 141.
(15) Antolini, L.; Battaglia, L. P.; Bonamartini Corradi, A.; Marcotrigiano, G.; Menabue, L.; Pellacani, G. C.; Saladini, M.; Sola, M. *Inorg. Chem.* **1986**, *25*, 2901.
(16) Gramaccioli, C. M.; Marsh, R. E. *Acta Crystallogr.* **1966**, *21*, 594.
(17) Brondino, C. D.; Casado, N. M. C.; Passeggi, M. C. G.; Calvo, R. *Inorg. Chem.* **1993**, *32*, 2078.

0020-1669/93/1332-6016$04.00/0

aspartate molecules are bridged by a Cu(II) ion. This extended-chain pattern is similar (and in fact simpler) to that found in the copper and zinc complexes of glutamic acid (glu), Cu(L-glu)-$(H_2O)_2$[16] and Zn(L-glu)$(H_2O)_2$[18] where each glutamic acid unit connects three metal ions (two equatorially and one apically). It is also similar to the ternary Cu(II) complexes of aspartic or glutamic acid with imidazole and 2,2'-bipyridine.[13,14,19] In these compounds the copper ions are bonded to the terminal carboxylate oxygen atoms of one molecule and to the residue carboxylate oxygen and nitrogen atoms of an adjacent aspartate molecule.

The magnetic susceptibility of Cu(L-asp)$(H_2O)_2$ shows a peak at about 7 K and decreases at lower temperatures (T). Its temperature dependence at low T fits well the behavior expected for antiferromagnetic one-dimensional chains with spins $S = {}^1/_2$. The g-tensor evaluated by EPR is related to the electronic structure around the copper ions and to the crystallographic arrangement. The variation of the EPR line width with the orientation of the magnetic field about the crystal axes and with microwave frequency is discussed in terms of the exchange interaction between copper ions.

Experimental Section

Sample Preparation. Cu(L-asp)$(H_2O)_2$ was obtained from the reaction of stoichiometric quantities of L-aspartic acid and copper basic carbonate in a water solution at 100 °C. The solution, taken to pH 5 by adding nitric acid, produced good single crystals when cooled to 10 °C in 1 day or after several days of slow evaporation at room temperature. They grow as thin sheets parallel to (100), elongated along b, with borders bounded by faces parallel to (001) and (010) planes. The weights of the largest single-crystal samples obtained up to this moment are less than 1 mg.

X-ray Diffraction Data. A data set was obtained at room temperature from a blue-green crystal with an Enraf-Nonius CAD-4 four-circle diffractometer, employing graphite-monochromated Mo Kα radiation. Unit cell parameters and the orientation matrix for data collection were obtained from 23 centered reflections in the range $10.2 < \theta < 25.1°$. Standard deviations of reflection intensities were calculated from counting statistics. The intensity of three standard reflections, (800), (080) and (008), monitored every 1800 s of radiation exposure, were essentially constant during the data collection. Data were corrected for Lorentz and polarization effects. An absorption correction, performed using the program DIFABS,[20] improved the R_{symm} agreement factor calculated for 29 pairs of symmetry-related reflections from 0.0135 to 0.0108. From the 830 reflections measured, 807 having $I > 3\sigma(I)$ were used for the structure determination and refinement. Scattering factors for bonded H atoms taken from Stewart *et al.*,[21] atomic scattering factors from Cromer and Waber,[22] and anomalous dispersion coefficients from Cromer and Ibers[22] for the rest of the atoms were used in the calculations. These were performed with the SHELX[23] and SDP[24] systems of programs. The stereoscopic projections shown were drawn with the programs ORTEP[25] and PLUTO.[26]

Magnetic Measurements. Magnetic susceptibility (χ) measurements in powdered samples of Cu(L-asp)$(H_2O)_2$ were performed with a DSM 8 susceptometer/magnetometer at a field of 10 kG and with a SHE, SQUID magnetometer at a field of 1 kG, in the range between 5 K and room temperature. Room-temperature EPR spectra of single crystals and powdered samples (made by crushing single crystals) were obtained at 9.7 and 33.4 GHz, using Bruker spectrometers equipped with 12-in. rotating electromagnets. The single crystal samples were glued to sample holders made of cleaved cubes of KCl single crystals, with the $\boldsymbol{a}$, $\boldsymbol{b}$ and $\boldsymbol{c}' = \boldsymbol{a} \times \boldsymbol{b}$ crystal directions parallel to the x, y and z axes of the cubes. These axes were taken as the laboratory reference systems. The sample holders were glued to an horizontal plane at the top of a pedestal that was positioned inside of the microwave cavities. This method allows to measure the EPR spectra for accurately known orientations of the magnetic field $\mathbf{H}$ in the xy, zx, and zy planes. A single, anisotropic resonance was observed for any orientation of $\mathbf{H}$. Its position and peak-to-peak line width were measured as a function of the orientation of $\mathbf{H}$, in three perpendicular planes xy (ab), zy ($c'b$), and zx ($c'a$) of the sample, at 9.7 and 33.4 GHz. Simulations of EPR spectra from powders were performed with a personal computer, considering the angular variations of the g-factor and the line width.

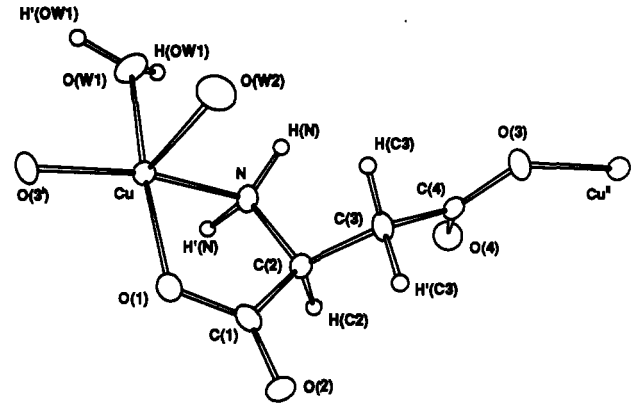

Figure 1. ORTEP projection of Cu(L-asp)$(H_2O)_2$ showing the atom-numbering scheme, the environment of the copper atom, and the aspartate molecule. The copper atom obtained from the first by a c translation is included in order to clarify the exchange interaction path between coppers.

Table I. Summary of Crystallographic Data for Cu(L-asp)$(H_2O)_2$

formula	$Cu(CO_2NH_2CHCH_2CO_2)(H_2O)_2$
mol wt	230.66
space group	$C2$
a	9.504(1) Å
b	10.038(3) Å
c	7.555(1) Å
β	94.01(2)°
v	719.0(2) Å^3
Z	4
radiation	Mo Kα, λ = 0.710 69 Å
temp	22 °C
linear abs coeff (μ)	3.04 mm^{-1}
$R = \sum\|\|F_o\| - \|F_c\|\|/\sum\|F_o\|$	0.0235
$R_w = [\sum w(\|F_o\| - \|F_c\|)^2/\sum w\|F_o\|^2]^{1/2}$	0.0253

Crystal Structure Determination and Refinement. The crystallographic data for Cu(L-asp)$(H_2O)_2$ are summarized in Table I. A full length table of crystallographic data is included in the supplementary material (Table S1). The structure was solved by standard Patterson and Fourier techniques and refined by full-matrix least-squares methods with anisotropic thermal parameters for all non-hydrogen atoms. All the hydrogen atoms on the L-aspartate ion and the two hydrogens of one water molecule were located from a difference Fourier map and incorporated in the molecular model. The positions of these atoms were refined with a common isotropic temperature parameter (which converged to $B = 3.2(5)$ Å^2) by fixing the bond distances to the corresponding atoms at their accepted values. A chirality test was performed by reversing all atomic coordinates and refining again to convergence. The R_w factor ($=[\sum w(|F_o| - |F_c|)^2/\sum w|F_o|^2]^{1/2}$) increased from 0.0318 to 0.0390.

Results and Discussion

Structural Results. Fractional coordinates and equivalent isotropic temperature parameters[27] for the non-H atoms in Cu-(L-asp)$(H_2O)_2$ are given in Table II. Relevant bond distances and angles around the copper ion are in Table III. Figure 1 is a drawing of the compound showing the labeling of the atoms.

(18) Gramaccioli, C. M. *Acta Crystallogr.* **1966**, *21*, 600.
(19) Antolini, L.; Marcotrigiano, G.; Menabue, L.; Pellacani, G. C.; Saladini, M.; Sola, M. *Inorg. Chem.* **1985**, *24*, 3621.
(20) Walker, N.; Stuart, D. *Acta Crystallogr.* **1983**, *A39*, 158.
(21) Stewart, R. F.; Davison, E. R.; Simpson, W. T. *J. Chem. Phys.* **1965**, *42*, 3175.
(22) Cromer, D. T.; Waber, J. T. In *International Tables for X-ray Crystallography*; Kynoch Press: Birmingham, England, 1974; Vol.IV, p 71. Cromer, D. T.; Ibers, J. A. *Ibid.*, p 149.
(23) Sheldrick, G. M. *SHELX, a Program for Crystal Structure Determination*; University of Cambridge: Cambridge, England, 1976.
(24) Frenz, B. A. *Enraf-Nonius Structure Determination Package*; Enraf-Nonius: Delft, The Netherlands, 1983.
(25) Johnson, C. K. *ORTEP. Report ORNL-3794*; Oak Ridge National Laboratory: Oak Ridge, TN, 1965.
(26) Motherwell, W. D. S.; Clegg, W. *PLUTO. A Program for Plotting Molecular and Crystal Structures*; Cambridge University; Cambridge, England, 1978.
(27) Hamilton, W. C. *Acta Crystallogr.* **1959**, *12*, 609.

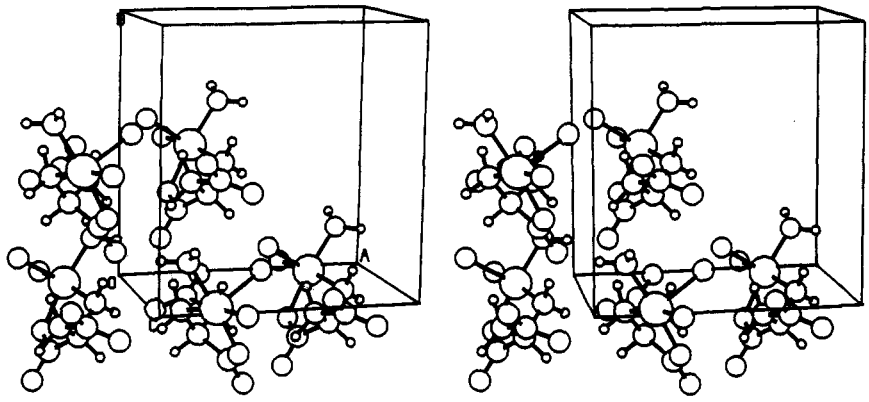

Figure 2. PLUTO stereoscopic projection of Cu(L-asp)$(H_2O)_2$ along *c*. The *b* axis is along the vertical. Dashed lines indicate H-bonds.

Table II. Fractional Atomic Coordinates and Isotropic Temperature Parameters (Å^2) of Cu(L-asp)$(H_2O)_2$

atom	*x/a*	*y/b*	*z/c*	B_{iso}
Cu	0.2365(0)	1.0000(0)	0.8746(1)	1.07(1)
O(1)	0.3291(3)	0.8281(3)	0.8464(4)	1.60(9)
O(2)	0.3903(3)	0.6829(3)	0.6450(4)	1.40(8)
O(3)	0.3070(3)	1.0085(5)	0.1230(3)	1.34(7)
O(4)	0.1185(3)	0.8925(3)	0.1900(4)	1.50(9)
O(W1)	0.1284(3)	1.1646(3)	0.8764(4)	1.72(9)
O(W2)	0.4278(3)	1.1139(4)	0.7766(5)	2.0(1)
N	0.1449(4)	0.9576(4)	0.6351(5)	1.14(9)
C(1)	0.3214(4)	0.7804(4)	0.6872(5)	1.2(1)
C(2)	0.2262(4)	0.8526(4)	0.5475(5)	1.1(1)
C(3)	0.3149(4)	0.9139(5)	0.4100(5)	1.2(1)
C(4)	0.2370(4)	0.9398(4)	0.2294(5)	1.0(1)

Table III. Interatomic Bond Distances (Å) and Angles (deg) for the Cu(II) Coordination Polyhedron in Cu(L-asp)$(H_2O)_2$[a]

(a) Bond Distances

Cu–O(1)	1.955(3)	Cu–O(W2)	2.313(3)
Cu–O(3^i)	1.950(2)	Cu–N	1.998(4)
Cu–O(W1)	1.946(3)		

(b) Bond Angles

O(1)–Cu–O(W1)	172.6(1)	O(W1)–Cu–N	89.4(1)
O(1)–Cu–O(W2)	91.8(1)	O(W1)–Cu–O(3^i)	95.9(1)
O(1)–Cu–N	83.4(1)	O(W2)–Cu–N	96.8(1)
O(1)–Cu–O(3^i)	90.9(1)	O(W2)–Cu–O(3^i)	93.5(1)
O(W1)–Cu–O(W2)	90.6(1)	N–Cu–O(3^i)	168.4(1)

[a] Symmetry code: (i) $x, y, z + 1$.

The anisotropic thermal parameters for the non-H atoms, the hydrogen atomic coordinates, bond distances and angles within the aspartate molecule, and some relevant least-squares planes and dihedral angles for the copper coordination polyhedron and the peptide molecule are provided as supplementary material. A stereoscopic view of the crystal packing is shown in Figure 2.

The Cu(II) ion is in a distorted tetragonal pyramidal coordination. At the corners of the pyramid base are an α-carboxylic oxygen [d(Cu–O) = 1.955(3) Å] and the amino nitrogen [d(Cu–N) = 1.998(4) Å] of one aspartate molecule, a β-carboxylic oxygen [d(Cu–O) = 1.950(2) Å] of another aspartate molecule (symmetry related by a translation along **c**), and a water molecule [d(Cu–OW) = 1.946(3) Å]. The 5-fold coordination is completed with a second water molecule at the top of the pyramid [d(Cu–OW) = 2.313(3) Å]. The Cu(II) ion is at 0.107(1) Å from the least-squares plane through the four atoms of the pyramid base, toward the apical water oxygen, whose distance from this plane is 2.418(3) Å.

Within the aspartate molecule, distances and angles are in agreement with literature values.[2] As expected, the Cα–COO atoms in the amino acid backbone are coplanar within experimental accuracy. This is also true for the residue Cβ–COO atoms. The dihedral angle between the corresponding least-squares planes is 85.9(1)°. The Cα–COO and Cβ–COO planes form angles of 10.0(6) and 85.9(1)°, respectively, with the least-squares plane through the base of the copper coordination pyramid.

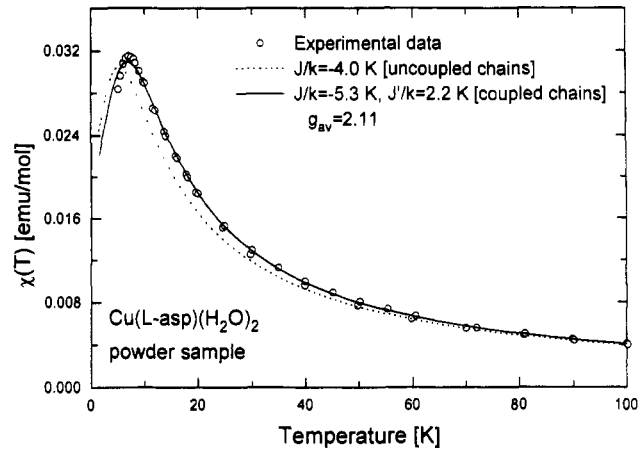

Figure 3. Magnetic susceptibility data of Cu(L-asp)$(H_2O)_2$. Dashed and solid lines are the predictions of models considering uncoupled antiferromagnetic copper chains with an intrachain coupling constant J/k = –4.0 K (eq 1) and antiferromagnetic chains with J/k = –5.3 K, ferromagnetically coupled to four neighboring chains, with an exchange coupling constant J'/k = 2.3 K (eq 2).

Table IV. Hydrogen Bond Distances (Å) and Angles (deg) for Cu(L-asp)$(H_2O)_2$[a,b]

D	H	A	D···A	H···A[d]	∠D–H···A[d]	D–H[d]
O(W1)	H(OW1)	O(2^{ii})	2.77	1.78	170.4	0.99
O(W2)	*c*	O(3^{iii})	2.79	*c*	*c*	*c*
O(W2)	*c*	O(4^{iv})	2.845	*c*	*c*	*c*
N	H(N)	O(2^{iv})	3.099	2.087	167.1	1.03
N	H′(N)	O(4^{v})	2.984	1.984	156.2	1.09

[a] Donor and acceptor atoms are indicated by D and A, respectively. All hydrogen bond distances with D···A and H···A distances up to 3.2 and 2.2 Å, respectively, are included. [b] Symmetry code: (ii) $x - 1/2, y + 1/2, z$; (iii) $1 - x, y, 1 - z$; (iv) $1/2 - x, y + 1/2, 1 - z$; (v) $-x, y, 1 - z$. [c] Presumed H-bonds as the hydrogen atoms of water molecule W2 could not be located in the final difference Fourier map (see text). [d] Standard deviations of distances and angles involving hydrogen atoms are not provided as in the refinement these atoms were kept at a fixed distance from the atom to which they are bonded (see text).

The aspartate ion, acting as a bidentate ligand, is attached to one Cu(II) ion, through the nitrogen and oxygen atoms of the α-carboxylate group (see Figure 1), and to another Cu(II) ion (symmetry related to the first one by a translation along **c**), through an oxygen atom of the residue β-carboxylate group. This generates covalently bonded –Cu–asp–Cu–asp–Cu– chains along the *c* axis. These chains are linked by interchain H-bond interactions involving the two water molecules and the amino group (see Figure 2). H-bond distances and angles are detailed in Table IV.

Magnetic Susceptibility. Figure 3 displays the susceptibility data $\chi(T)$ for Cu(L-asp)$(H_2O)_2$ as a function of temperature *T*,

for $T \leq 100$ K, where most of the data points were taken. These data points have been corrected for the diamagnetic contribution using the Pascal constants. A predominant antiferromagnetic Curie–Weiss behavior of the high-temperature data is observed and is compared to

$$[\chi(T)]^{-1} = \frac{T - \Theta_c}{C_m}$$

A least-squares analysis of the data between 20 and 100 K gives the parameters $C_m = 0.417$ emu/mol and an antiferromagnetic Curie temperature $\Theta_c = -1.9$ K. This value of C_m leads to an average g-factor $g = 2.11$.

The data in Figure 3 display a rounded maximum around 7 K and decreasing values of $\chi(T)$ at lower temperatures. No indication of a magnetic phase transition is observed. The maximum in $\chi(T)$ suggests short-range order, typical of low-dimensional magnetic systems. The data were analyzed using the Heisenberg model with exchange interaction between pairs of Cu(II) ions with spins $\mathbf{S}_i$ and $\mathbf{S}_j$ of the form

$$\mathcal{H} = \sum_{i>j} \mathcal{H}_{ij} = \sum_{i>j} -2J_{ij}\mathbf{S}_i\cdot\mathbf{S}_j$$

where we assumed interaction only between nearest neighbors copper ions on a chain (i.e., $J_{ij} = J$, for $j = i \pm 1$, and $J_{ij} = 0$ otherwise). We analyzed the data in terms of the empirical function

$$\chi_c(T) = \frac{Ng^2\mu_o^2}{|J|}\left[\frac{0.25x + 0.14995x^2 + 0.30094x^3}{1 + 1.9862x + 0.66854x^2 + 6.0626x^3}\right] \quad (1)$$

where $x = |J|/kT$, N and k are the Avodagro and Boltzmann constants, μ_o is the Bohr magneton, and g is the averaged g-factor. Equation 1 is a slightly modified version of the algebraic function introduced by Hatfield and collaborators[28] to represent the numerical calculations performed by Bonner and Fisher,[29] describing a uniformly spaced chain of spins with $S = {}^1/_2$. The term within brackets in eq 1 has a maximum value 0.073 56 at $x_{max} = 0.7725$ ($T_{max} = 1.294|J|/k$). In order to reproduce the experimental result $\chi_{max} = 0.031$ emu/mol observed at $T_{max} \approx 7$ K using $g = 2.11$, the value of $|J|/k$ must be close to 4 K. In fact, a least-squares fitting of eq 1 to the data in Figure 3 gives $J/k = -4.0$ K (antiferromagnetic). The values of $\chi_c(T)$ calculated with this value of J and eq 1 are displayed in Figure 3 as a dashed line. They show the general behavior of the data, but the values calculated are shifted to lower temperatures in the low-T range.

The crystal structure of Cu(L-asp)$(H_2O)_2$ suggests that the Cu(II) magnetic chains just described are the asp–Cu–asp–Cu–asp chains described before. Then, the paths for superexchange between neighboring copper ions on a chain are provided by the σ bonding along the skeleton of the aspartic acid molecule (see Figure 1). Since the chains are not isolated, we introduced interchain interactions in a mean field approximation, using[30]

$$\chi(T) = \frac{\chi_c}{1 - 2zJ'\chi_c/Ng^2\mu_o^2} \quad (2)$$

where $\chi_c(T)$ is the susceptibility for the uncoupled chains given by eq 1, z is the number of nearest copper neighbors in adjacent chains ($z = 4$ in our case) and J' is the interchain exchange parameter. By this method we obtain $J/k = -5.3$ K for the antiferromagnetic exchange within a chain and a ferromagnetic $J'/k = +2.2$ K for the mean value of the ferromagnetic interchain exchange interaction. These values and eqs 1 and 2 produce the solid curve included in Figure 3. The agreement of this curve with the experimental data is better than that of the dashed curve in Figure 3, obtained considering only intrachain interactions. Furthermore, the value of the exchange interaction averaged over the six nearest neighbors (two in the same chain and four in neighbor chains) is negative, therefore supporting the value and the sign of the antiferromagnetic Curie temperature Θ_c obtained above.

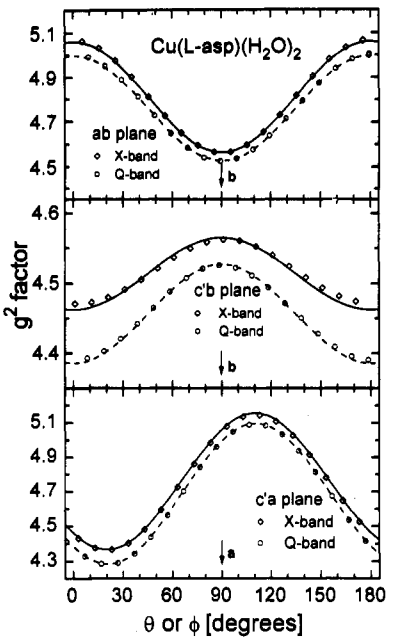

Figure 4. Angular variation of the squared g-factor measured at 9.7 and 33.4 GHz at room temperature, in three orthogonal planes of single-crystal Cu(L-asp)$(H_2O)_2$. The curves were obtained by least-squares fitting of the data at each microwave frequency with a symmetric second-order $\mathbf{g}^2$ tensor. The eigenvalues and eigenvectors obtained for $\mathbf{g}^2$ are given in Table V.

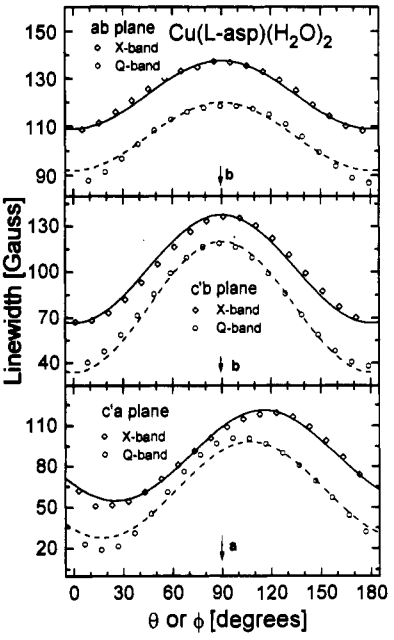

Figure 5. Angular variation of the peak-to-peak EPR line width of Cu(L-asp)$(H_2O)_2$ measured at 9.7 and 33.4 GHz and room temperature with the magnetic field applied in three orthogonal planes. The curves were obtained by a least-squares fitting of eq 4 to the data.

EPR Data. The values of the squared g-factor $g^2(\theta,\varphi)$ of the single line observed for a magnetic field $\mathbf{H}$ applied in the three studied crystal planes of Cu(L-asp)$(H_2O)_2$, at 9.7 and 33.4 GHz, are displayed in Figure 4a-c. The peak-to-peak line width ΔH data are in Figure 5a-c.

(28) Hall, J. W. Ph.D. Dissertation, University of North Carolina, Chapel Hill, 1977. Hatfield, W. E. *J. Appl. Phys.* **1981**, *52*, 1985.
(29) Bonner, J. C.; Fisher, M. E. *Phys. Rev.* **1964**, *A135*, 640.
(30) Hatfield, W. E.; Weller, R. R.; Hall, J. W. *Inorg. Chem.* **1980**, *19*, 3825.

Table V. Values of the Eigenvalues and Eigenvectors of the g^2 tensor for Cu(L-asp)$(H_2O)_2$, Molecular g-factors $g_\parallel$ and $g_\perp$, Polar (θ_M) and Azimuthal (φ_M) Angles of the Molecular Axis at One Site in the (xyz) ≡ ($a'bc$) Reference System, and Angle 2α between the Molecular Axes of the Two Copper Sites, As Obtained from The EPR Data,[a] and Parameters of the Expansion of the Angular Variation of the Line Width (Eq 7)

	9.7 GHz	33.4 GHz	calcd
	(a) Eigenvalues and Eigenvectors of the **g**-Tensor		
g_1	2.091(1)	2.094(1)	
g_2	2.137(1)	2.128(1)	
g_3	2.270(1)	2.258(1)	
V_1	(0,1,0)	(0,1,0)	
V_2	(0.342,0,0.940)	(0.352,0,0.936)	
V_3	(0.940,0,–0.342)	(0.936,0,–0.352)	
	(b) Molecular g-Values		
$g_\parallel$	2.312(1)	2.311(1)	
$g_\perp$	2.089(2)	2.070(2)	
θ_M (deg)	108(1)	108(1)	110.3
ϕ_M (deg)	28(1)	30(1)	30.8
2α (deg)	126(1)	123(1)	122.6
	(c) Coefficients of the Second-Order Expansion of $\Delta H(\theta,\varphi)$ (eq 5)		
a_{11}	109.1(5)	92(1)	
a_{22}	137.6(5)	120(1)	
a_{33}	66.8(5)	34(1)	
$a_{12} = a_{23}$	0(1)	0(1)	
a_{13}	–26.5(5)	–20(1)	

[a] The values of (θ_M,ϕ_M) and 2α, calculated from the crystallographic data, are included in the last column for comparison.

g-Factor. The variation of the position of the EPR line with the orientation of the magnetic field is described by the spin hamiltonian $H = \mu_B \mathbf{H}\cdot\mathbf{g}\cdot\mathbf{S}$, where μ_B is the Bohr magneton, **S** the effective spin ($S = {}^1/_2$), and **g** the crystal g-tensor. The components of the tensor $\mathbf{g}^2 = \mathbf{g}\cdot\mathbf{g}$ were evaluated at each microwave frequency by least-squares fitting of the data in Figure 4a-c with the function $g^2(\theta,\varphi) = \mathbf{h}\cdot\mathbf{g}\cdot\mathbf{g}\cdot\mathbf{h}$, where $\mathbf{h} = \mathbf{H}/|\mathbf{H}|$= (sin θ cos φ,sin θ sin φ, cos θ) defines the direction of **H** in the system **x, y, z** ≡ **a, b, c'** of the sample. The values of the eigenvalues and eigenvectors of $\mathbf{g}^2$ obtained from these components are given in Table V. This tensor, which turns out to have rhombic symmetry, explains well the observed angular variation of $g^2(\theta,\varphi)$ at both frequencies as shown by the solid lines in Figure 4a-c.

Our results for the eigenvalues of the observed **g**-tensor (Table V) differ from those obtained by Antolini *et al.*[13] from the powder EPR spectra of the same compound. These authors report axial symmetry with $g_\parallel$= 2.249 and $g_\perp$ = 2.076. To explain the differences, we display in Figure 6 the EPR spectrum of a powder sample of Cu(L-asp)$(H_20)_2$ obtained at 9.7 GHz. We include in this figure a simulated spectrum calculated with the parameters obtained from our single-crystal experiments (g-factors and line widths of Figures 4 and 5). As indicated by arrows in Figure 6, even if the two peaks of the powder spectrum correspond to the g-factors reported in ref 13, they do not give an accurate representation of the eigenvalues of $\mathbf{g}^2$. This is attributed to the line width anisotropy, which cannot be considered in the analysis of powder data. Therefore, the discrepancy can be traced to the limitations inherent to the procedure of extracting information from EPR spectra of powdered samples.[31]

The single EPR line observed for Cu(L-asp)$(H_2O)_2$ corresponds to a collective resonance of the copper ions in the lattice. The four symmetry-related copper sites per unit cell can be grouped into two pairs of sites. Copper ions within each pair are related by the *C* centering lattice translation and therefore should give identical EPR spectra. Different pairs of copper sites are related through a 2-fold axis along **b**. They will be called sites A and B, are magnetically nonequivalent, and should give rise to two different EPR resonances for **H** neither along the **b** axis nor perpendicular to it. The single resonance observed in the *ab* and *bc* planes (Figure 4a,b) arises from the collapse of the resonances expected from sites A and B, due to exchange interaction coupling magnetically nonequivalent Cu(II) ions.[32] The hyperfine coupling with the copper nuclei and with the ligands are also averaged out by the exchange. In fact, the analysis of the susceptibility data given above indicates that the condition $|J'| \geq {}^1/_2|g_A - g_B|\mu_B H$, needed to collapse the resonances corresponding to Cu(II) ions in sites A and B (then in different chains) is fulfilled. Then, the observed resonance should correspond to a tensor **g** average of the molecular **g**-tensors $\mathbf{g}_A$ and $\mathbf{g}_B$ for copper ions at sites A and B.

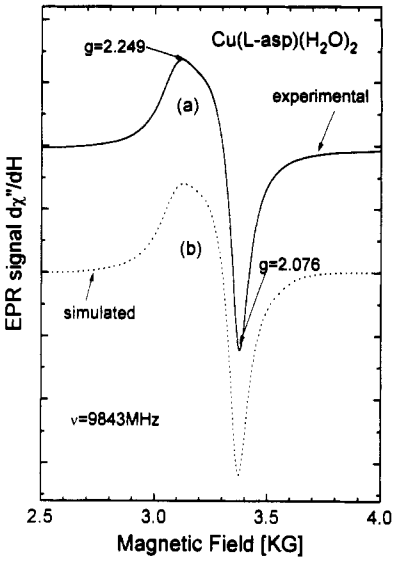

Figure 6. (a) Observed EPR spectrum of powdered Cu(L-asp)$(H_2O)_2$ at 9.7 GHz and room temperature. (b) Simulated EPR spectrum, calculated using the $\mathbf{g}^2$ tensor and the coefficients in the expansion of the line width $\Delta H(\theta,\varphi)$ (eq 3), given in Table V.

Assuming axial symmetry around the copper ions, and using the method described in refs 33-35, we obtained from the components of the observed $\mathbf{g}^2$ tensor the molecular g-values $g_\parallel$ and $g_\perp$, the orientation (θ_M,φ_M) of the molecular axis for one copper site in the unit cell of Cu(L-asp)$(H_2O)_2$, and the angle 2α between the axes of the two magnetically nonequivalent copper sites. This information is given in Table V. There, they are compared with the orientation (θ_M,φ_M) of the normal to the plane of equatorial ligands and the angle 2α between the axes of the two copper sites, calculated from the structural data. The good agreement between these values and those calculated from the EPR data supports the assumption of axial symmetry around copper ions. The values $g_\parallel$ = 2.312 (2.311) and $g_\perp$ = 2.089 (2.070) of the molecular g-factors, calculated from the data at 9.7 GHz (33.4 GHz), characterize the orbital ground state of the unpaired electron. They are larger than those corresponding to copper–amino acid (aa) complexes of the Cu$(aa)_2$ or bis(glycine)copper type measured previously, where $g_\parallel \approx 2.25$ and $g_\perp \approx 2.06$.[34-37] The main difference between these complexes, concerning the environment around the Cu(II) ion, consists in the replacement of the equatorial water oxygen in Cu(L-asp)$(H_2O)_2$ (see Figure 1) by an amino nitrogen atom in the Cu$(aa)_2$ compounds. We attribute the larger values of the g-factors in Cu(L-asp)$(H_2O)_2$

(31) Pilbrow, J. R. *Transition Ion Electron Paramagnetic Resonance*; Clarendon Press, Oxford, England, **1990**; Chapter 5.

(32) Bencini, A.; Gatteschi, D. *Electron Paramagnetic Resonance of Exchange Coupled Systems*; Springer: Berlin, Germany, 1990.

(33) Billing, D. E.; Hathaway, B. J. *J. Chem. Phys.* **1969**, *50*, 1476. Hathaway, B. J.; Billing D. E. *Coord. Chem. Rev.* **1970**, *5*, 143.

(34) Calvo, R.; Mesa, M. A. *Phys. Rev. B* **1983**, *28*, 1244.

(35) Calvo, R.; Isern, H.; Mesa, M. A. *Chem. Phys.* **1985** *100*, 89.

(36) Hoffmann, S. K.; Gozlar, J.; Sczepaniak, L. S. *Phys. Rev. B* **1988**, *37*, 7331.

(37) Steren, C. A.; Calvo, R.; Castellano, E. E.; Fabiane, M. S.; Piro, O. E. *Physica B* **1990**, *164*, 323.

to the bigger electronegativity of this water molecule compared to the nitrogen atom. This produces two effects: first, a decrease of the cubic field and therefore smaller energy differences $\Delta E_{xy} = E_{xy} - E_{x^2-y^2}$ and $\Delta E_{zx} = E_{zx} - E_{x^2-y^2}$ between the d(xy) and d(zx) orbital states and the ground d($x^2 - y^2$) orbital state of Cu(L-asp)$(H_2O)_2$; second, a less delocalized magnetic orbital. As shown in refs 38 and 39, for a copper ion in a square planar coordination of ligands,

$$g_\parallel = g_o + 8\frac{|\lambda|\alpha\alpha_1}{\Delta E_{xy}} \qquad g_\perp = g_o + 2\frac{|\lambda|\alpha\beta_2}{\Delta E_{zx}}$$

where $g_o = 2.0023$, λ is the spin–orbit coupling constant, and α, α_1, and β_2 are the mixing parameters for the molecular orbitals.[38,39] The replacement of a nitrogen ligand by the water oxygen decreases ΔE_{xy} and ΔE_{zx} and increases α, α_1, and β_2, producing in both cases an increase of $g_\parallel$ and $g_\perp$. In fact, the molecular g-values obtained for Cu(L-asp)$(H_2O)_2$ (Table V) are similar to those measured by Bonomo *et al.*[40] for copper impurities in Cd(L-glu)$(H_2O)_2$ and by Brondino *et al.*[17] for copper impurities in Zn(L-glu)$(H_2O)_2$ ($g_x = 2.0678$, $g_y = 2.0920$, $g_z = 2.3545$ and $g_x = 2.053$, $g_y = 2.089$, $g_z = 2.345$, respectively). The g-values are also similar to those calculated from the EPR data in Cu(L-glu)$(H_2O)_2$ using a method similar to that used here for Cu(L-asp)$(H_2O)_2$.[17] In those systems the local arrangement around the Cu(II) ions is similar to that found in Cu(L-asp)$(H_2O)_2$, with a water oxygen atom as an equatorial ligand. To be in accord with this idea, the ternary copper complexes of L-aspartic and L-glutamic acid with imidazole, 2,2′-bipyridine and 1,10-phenanthroline, where the equatorial water oxygen is replaced by the amine ligand, should show $g_\parallel \approx 2.25$ and $g_\perp \approx 2.06$. The g-values obtained by Antolini *et al.*,[13-15,19] from data of powdered samples, show both kinds of behavior and therefore are inconclusive in this respect. However, in view of the above mentioned uncertainties in the interpretation of EPR data from powdered samples, single crystal experiments are needed to confirm the results in these systems.

EPR Line-Width. Assuming an angular dependence of the line width given by the quadratic form $\Delta H = \mathbf{h}\cdot\mathbf{a}\cdot\mathbf{h}$, where $\mathbf{a}$ is a symmetric second-order tensor, the experimental data in Figure 5 were least-squares fitted with the function

$$\Delta H(\theta,\varphi) = a_{11}\sin^2\theta\cos^2\varphi + a_{22}\sin^2\theta\sin^2\varphi + a_{33}\cos^2\theta + 2a_{12}\sin^2\theta\sin\varphi\cos\varphi + 2a_{13}\sin\theta\cos\theta\cos\varphi + 2a_{23}\sin\theta\cos\theta\sin\varphi \quad (3)$$

The a_{12} and a_{23} components of the $\mathbf{a}$ tensor should vanish because of crystal symmetry. These and the other least-squares coefficients a_{ij} calculated at each microwave frequency are included in Table V. Contributions to the line width due to dipole–dipole interactions in a one-dimensional magnet[41] were not observed. This is expected because of the large magnitude of the interchain interactions indicated by the susceptibility data. The solid lines displayed in Figure 5 are obtained with these values. Figure 5 shows that the line width *decreases* with increasing microwave frequency. This suggests important nonsecular contributions at 9.7 GHz. Different behavior may be expected for a paramagnetic crystal with magnetically nonequivalent sites A and B.[42] In this case, the information about the difference in the molecular $\mathbf{g}$-tensors $\mathbf{g}_A$ and $\mathbf{g}_B$ is lost because of the exchange averaging effect and may appear as a frequency-dependent contribution to the line width. This contribution *increases* ΔH as ω_o^2 at higher microwave frequencies ω_o and is described by[42]

$$\Delta H_{AB}(\theta,\varphi) = \sqrt{\frac{2\pi}{3}}\frac{[g_A(\theta,\varphi) - g_B(\theta,\varphi)]^2\hbar\omega_o^2}{4g^3(\theta,\varphi)\omega_{ex}\mu_B} \quad (4)$$

where the exchange frequency ω_{ex} is proportional to $|J'| = |J_{AB}|$. This contribution was observed in Cu(L-glu)$(H_2O)_2$·[17] where adjacent Cu(II) ions on a –glu–Cu–glu–Cu–glu– chain are related by a C_2 axis. This fact allowed us[17] to evaluate from EPR line width data the magnitude $|J_\sigma/k| = |J_{AB}|/k = 0.19$ K for the exchange interaction between neighboring coppers connected through the σ skeleton of the glutamic acid molecule. To this purpose, we extracted from the observed $\Delta H(\theta,\varphi)$ the component proportional to $[g_A(\theta,\varphi) - g_B(\theta,\varphi)]^2$ at each of the two different microwave frequencies. In Cu(L-asp)$(H_2O)_2$, where rotated copper atoms are in different chains, the observed (small) decrease of ΔH with ω_o sets a lower limit to the exchange coupling constant $J' = J_{AB}$. Considering the difference $(g_A - g_B)^2$ calculated with the molecular $\mathbf{g}$-tensors, and using eq 4, we estimate $|J'|/k \geq 0.5$ K, in agreement with the result obtained from the susceptibility data. As in the analysis of these data, we assume that there are four equivalent copper ions of the B type nearest neighbors to a given copper ion of the type A.

Polymeric Structure and Exchange Paths in Cu(L-asp)$(H_2O)_2$. The polymeric structure of Cu(L-glu)$(H_2O)_2$[16] and Cu(L-asp)$(H_2O)_2$ is due to the presence of a second carboxylate group in the glutamic and aspartic acid molecules, respectively. These molecules connect two copper ions in Cu(L-asp)$(H_2O)_2$ and three in Cu(L-glu)$(H_2O)_2$ through the oxygens of the α- and β- (or γ-) carboxylate groups. This has been discussed by Antolini *et al.*[13-15] in their studies of the ternary copper complexes of L-glu and L-asp with imidazole, bipyridine, and phenanthroline. They conclude that low or nonhydrated ternary complexes are of the polymeric type, while highly hydrated compounds are of the molecular type. Water molecules bonded to the Cu(II) ion may preclude binding of copper to two (or more) carboxylate oxygens.

The polymeric structure of Cu(L-asp)$(H_2O)_2$ is responsible of the spin chain magnetic behavior displayed by the susceptibility data. The value $J/k = -5.3$ K for the exchange interaction between nearest copper neighbors in these chains is assigned to copper pairs connected in an equatorial fashion to L-aspartic acid molecules. As shown in Figures 1 and 2, this path in Cu(L-asp)$(H_2O)_2$ involves the glycine ring plus *four* diamagnetic atoms. This result may be compared with that for Cu(L-glu)$(H_2O)_2$,[17] where $|J_\sigma/k| = 0.19$ K was obtained by EPR for the magnitude of the exchange interaction between coppers equatorially connected by L-glutamic acid molecules. This path involves the glycine ring plus *five* diamagnetic atoms. The 1 order of magnitude difference could be attributed not only to the longer length of the σ skeleton of glutamic acid but also to the angles between the bonds involved in each case. No calculations that could be compared with these results have been performed yet.

The value $J'/k = 2.2$ K obtained from the susceptibility data for the interchain interaction is a mean value over the magnetic interactions between a given copper ion and the nearest copper ions in each of the four adjacent chains. It is not much smaller than the intrachain interaction J/k, and then the mean field model used[30] introduces an uncertainty in the evaluation. A copper ion on a given chain of Cu(L-asp)$(H_2O)_2$ has four magnetically nonequivalent copper neighbors at 5, 5.2, 5.4, and 5.4 Å, located on the four chains of the rotated type in close contact with the first chain and interacting with it through a net of hydrogen bonds. These contacts provide the paths for superexchange interactions between chains (of coupling constant J'). It is interesting to note that J' is larger (and of different sign) than the magnitudes of the exchange interaction through hydrogen bonds reported in Cu(L-but)$_2$ and Cu(D,L-but)$_2$ (–0.64 and –0.84 K, respectively), calculated from specific heat data.[8] This may seem surprising since the hydrogen bonds in Cu(L-asp)$(H_2O)_2$

(38) Maki, A. H.; McGarvey, B. R. *J. Chem. Phys.* **1958**, *29*, 31 and 35.
(39) Kivelson, D.; Neiman, R. J. *J. Chem. Phys.* **1961**, *35*, 149.
(40) Bonomo, R. P.; Pilbrow, J. R.; Sinclair, J. R. *J. Chem. Soc., Dalton Trans.* **1983**, 489.
(41) Richards, P. M. in *Local Properties at Phase Transitions;* Editrice Compositori: Bologna, Italy, 1975.
(42) Levstein, P. R.; Steren, C. A.; Gennaro, A. M.; Calvo, R. *Chem. Phys.* **1988**, *120*, 449.

do not bridge oxygen atoms directly bonded to the copper ions (i.e., the oxygens in the NO_3 planar arrangement of equatorial ligands). In one case they connect the apical water oxygen of one copper to one equatorial oxygen of the neighbor copper. In the other cases the coupling paths are more complex and involve hydrogen bonds and carboxylate bridges; they connect an equatorial nitrogen or water oxygen of one copper to an equatorial carboxylate oxygen of the neighbor copper. In the cases of Cu(L-but)$_2$ and Cu(D,L-but)$_2$, the superexchange paths are hydrogen bonds connecting oxygen and nitrogen atoms equatorially bonded to copper. It seems that the overlap integral of the magnetic orbitals connecting different chains in Cu(L-asp)$(H_2O)_2$ is very small, and then the ferromagnetic interaction is predominant. The larger overlap of the magnetic orbitals in Cu(L-but)$_2$ and Cu(D,L-but)$_2$ introduces a larger antiferromagnetic contribution.[43,44]

Concluding Remarks. This is the first report on the structural and magnetic properties of a new interesting material, Cu(L-asp)$(H_2O)_2$. Due to the bonding characteristics of aspartic acid, this material forms polymeric chains asp–Cu–asp–Cu–asp, with long but effective exchange paths provided by the σ skeleton of the amino acid. A transition to 3D magnetic order is not observed in the powder susceptibility data above 5 K even if the interchain couplings are relatively large. As explained by Landee et al.,[45] susceptibility measurements in single-crystal samples and at lower temperatures may give clues on the anisotropy of the exchange interaction and about possible phase transitions. Up to this moment these have been precluded by the small size of the single crystals obtained. Specific heat measurements as those performed in other copper amino acid complexes[7,8] are planned.

Acknowledgment. We are grateful to G. Ferreyra for growing some of the single-crystal samples studied. The EPR measurements at 33.4 GHz were performed at the Magnetic Resonance Laboratory, Centro Atómico Bariloche, Argentina. We thank A. Butera and L. B. Steren for valuable help during these measurements. This work was supported by Grants 3–098600, 3–071300, and 3–907602 of the Consejo Nacional de Investigaciones Científicas y Técnicas (CONICET), by a binational grant of the Fundación Antorchas of Argentina, and by the Conselho Nacional de Pesquisas (CNPq), the Fundação de Amparo a Pesquisa do Estado de São Paulo (FAPESP), and the Financiadora de Estudos e Projetos (FINEP) of Brazil. R. C. and O. E. P. thank FAPESP for financial support during visits to the IFQSC, USP, Brazil.

Supplementary Material Available: Complete crystallographic data (Table S1), anisotropic thermal parameters for the non-hydrogen atoms (Table S2), fractional coordinates of the hydrogen atoms (Table S3), distances and angles for the Cu(II) coordination sphere and within the aspartate molecule (Table S4), and least-squares planes and dihedral angles (Table S5) (5 pages). Ordering information is given on any current masthead page.

(43) Anderson, P. W. In *Magnetism*; Rado, G. T., Suhl, H., Eds., Academic Press: New York, 1963; Vol. 1.
(44) Hay, P. J.; Thibeault, J. C.; Hoffmann, R. *J. Am. Chem. Soc.* **1975**, *97*, 4884.
(45) Landee, C. P.; Lamas, A. C.; Greeney, R. E.; Bucher, K. G. *Phys. Rev. B* **1987**, *35*, 228 and references therein.